Trees, Forests and People 17 (2024) 100627

Contents lists available at ScienceDirect

Trees, Forests and People

journal homepage: www.sciencedirect.com/journal/trees-forests-and-people

Taper functions to predict the upper stem diameter of Chir pine (*Pinus roxburghii*) in the mid-hills of Nepal

Pradip Saud [a,b,*], Tolak R. Chapagain [c,*], Shes K. Bhandari [d], W. Keith Moser [e]

[a] *Arkansas Forest Resource Center; College of Forestry, Agriculture, and Natural Resources, University of Arkansas at Monticello, 110 University Court, Monticello, AR 71656, USA*
[b] *Arkansas Center for Forest Business, University of Arkansas at Monticello, Monticello, AR 71656, USA*
[c] *Province Forest Directorate, Butwal, Lumbini Province, Nepal*
[d] *Institute of Forestry, Pokhara Campus, Tribhuvan University, Nepal*
[e] *Rocky Mountain Research Station, Forest Service, US Department of Agriculture, 2500 S. Pine Knoll Dr., Flagstaff, AZ 86001, USA*

ARTICLE INFO

Keywords:
Maximum likelihood
Mixed-effects model
Autocorrelated errors
Variance function matrix
K-fold cross-validation

ABSTRACT

A function that predicts the upper stem diameters of an individual tree is helpful in better quantifying the volume and devising sustainable management of commercially and ecologically important species. This study compares three forms of the taper equation (single, variable-exponent, and segmented) using destructive sample data collected from 80 Chir pine (*Pinus roxburghii* Sarg.) trees across three adjacent stands in the Mid hills of Nepal. A mixed-effects modeling approach was used to evaluate the 13 different taper functions, selecting the best parameter association with the random effect to avoid overparameterization. Additionally, these models were fitted to minimize errors by modeling correlation structure with continuous autoregressive correlation structure of order 1 (corCAR1) and variance with a power variance function. All models were statistically significant at 5% level in the likelihood ratio test when compared with the models fitted without these error minimization. Furthermore, model performance (root mean square error, mean absolute error, and pseudo-R^2) was evaluated using k-fold cross-validation procedure. Although all taper functions described more than 95% of the variation in upper stem diameter prediction, the single-form models of Bennett and Swindel (1972) and Amidon (1984), the variable-exponent model form of Sharma and Zhang (2004), and the segmented model form of Max and Burkhart (1976) explained more than 98% percent of the variability. Residual diagnostics indicated that Sharma and Zhang's (2004) model provided better constant and minimum errors in predicting the upper stem diameter along the 8 to 20 m stem length, whereas other models exhibited higher residual errors. Despite model's better performance, variability along the upper stem diameter prediction would affect its applicability in estimating the volume at any merchantable height of individual trees.

1. Introduction

The stem taper function, an allometric growth model, utilizes the measurements of total height (H), diameter at breast height (D), and height (h) above the ground at which upper stem diameter (d) is measured to estimate the rate of change in diameter with increasing height along the tree stem (Kozak et al., 1969; Max and Burkhart, 1976; Ormerod, 1973; Pain and Boyer, 1996; Cao, 2009; Sharma and Parton, 2009; Lynch et al., 2017). Integration of taper equations allows for predicting upper stem diameter, estimating accurate total volume, and predicting timber yield, which is crucial for economic planning of forestry operations and sustainable forest management (Garber and Maguire, 2003; Sharma and Zhang, 2004; Lynch et al. 2017). These equations also estimate biomass and carbon stocks in forests, which are critical for understanding the role of forests in carbon sequestration and climate change mitigation (Cao and Wang, 2011; Zhao et al., 2019).

Despite the development of many taper functions, their successful applications have been limited due to variability in species and stem shapes (Sharma and Zhang, 2004; Rojo et al., 2005; Arias-Rodil et al., 2015; Arias-Rodil et al., 2017; Poudel et al., 2018). This variability is often complex due to the stand characteristics that introduce challenges in accurately defining tree form to predict the total and merchantable volumes at any given height from the stump height (Farrar and Murphy, 1987; Clark et al., 1991; Jiang et al., 2007; Sharma and Parton, 2009;

* Corresponding authors.
E-mail addresses: saud@uamont.edu (P. Saud), chapagain.tolak@gmail.com (T.R. Chapagain).

https://doi.org/10.1016/j.tfp.2024.100627

Available online 14 July 2024

Ulak et al., 2022). Considering the region and tree species type, numerous complex model forms have been attempted worldwide to describe stem taper compatible for volume estimation, ranging from simple to variable-exponent and segmented taper models. Over time, these taper equation have been modified by imposing conditions to reduce bias and provide a more accurate prediction for different tree species.

A simple taper function (Behre, 1923) has been modified from quadratic (Matte, 1949) to a polynomial function (Kozak et al., 1969; Ormerod, 1973; Demaerschalk, 1972; Clutter, 1980) to become compatible with existing local volume equations. These simple taper equations are commonly used to develop local volume tables. The variable-exponent taper equation considers an individual tree form. It describes the stem profile as a single continuous function, adjusting the exponent from the ground to the top to represent the neiloid, paraboloid, and other intermediate forms (Kozak, 1988; Riemer et al., 1995; Sharma and Zhang, 2004; Poudel et al., 2018). Furthermore, the segmented taper equation, which uses a step function, characterizes the entire stem profile and reduces the bias by dividing the stem length into multiple segments at inflection points (Max and Burkhart, 1976; Goulding and Murray, 1976; Cao et al., 1980; Demarschalk and Kozak, 1977). This segmented taper model uses different sets of model joints for the various parts of the stem such that merchantable and total volume can be easily estimated by direct integration of the taper equation (Max and Burkhart, 1976; Fang et al., 2000; Cao et al., 1980; Cao and Wang, 2015; Sabatia et al., 2015). Conversely, variable-exponent taper functions require some algebraic adjustments to establish the taper and volume relationship because the models are developed empirically rather than being geometrically compatible for integration (Clutter, 1980; Amidon, 1984; Gordan, 1983; Lynch et al., 2017; Zhao and Kane, 2017; Zhao et al., 2019).

Using separate sets of equations, such as cylindrical volume for stump and cone volume for top sections, and Smalian's formula for the middle section, the volume of a tree can be easily estimated. To improve volume estimation by providing better parameter estimates for the prediction of upper stem diameter (d), the modeling of these taper equations has considered the mixed-effects modeling approach. This approach models the covariance structure of random effects and random errors (Cao and Wang, 2011; Arias-Rodil et al., 2015; Saud et al., 2019; Zhao et al., 2019). Model fitting for the taper equation violates the independence assumption because data are taken at the multiple measurement points on each sample stem, leading to correlated observations. Multiple d measurements at varying heights (h), that vary with taperness and proportionality to D introduce autocorrelated errors and provide weight of D, resulting *in* variability in residual errors. The mixed-effects approach accounts for the correlation between the successive measurements on the same tree and the heteroscedasticity error by modeling the covariance matrix in predicting d as the random effects component and the within-subject component and provides better parameter estimations of a taper equation (Garber and Maguire, 2003; Yang et al., 2009; Gómez-García et al., 2013; Zhao et al.. 2019; Hussain et al., 2020).

Chir pine (*Pinus roxburghii* Sarg.), a widely distributed evergreen conifer species, is one of the dominant tree species in subtropical forests of the Indo-Pacific region (Singh and Kushwaha, 2011; Bisht et al., 2014). It extends from Bhutan to the western Himalayas, at elevations ranging from 450 m to 2300 m above sea level. In Nepal, the Chir pine forest is distributed in the subtropical region at altitudes ranging from 1000 m to 2000 m (Jackson, 1994) and contributes 7.05% (11.62 m^3 ha^{-1}) in total standing volume and 8.45% in forest-type coverage (DFRS, 2015). This forest type is intensively managed for resin tapping and timber production, such as building construction and furniture making. Resin tapping from the trunk of living Chir pine trees is a commercial activity that contributes to local community income and the national economy (Paudyal, 2008). Additionally, Chir pine forest enhances ecosystem services, such as carbon sequestration, greenery, and soil conservation (Sharma et al., 2020).

Although studies on modeling the growth and yield of Chir pine forest began in the early 1980s, only a few models are available to the scientific community. For example, total and merchantable volume equations (Joshi, 1984), biomass prediction model for a plantation stand (Joshi, 1985), and volume equations and biomass prediction models (Sharma and Pukkala, 1990). However, some models are either unavailable to the scientific community or limited to generating stem volume tables from diameter and height measurements. For example, the volume prediction model by Sharma and Pukkala (1990) is based on timber volume to 10 cm (4 inches) and 20 cm (8 inches) top diameter measurements, and total height. Other studies include the evaluation of the growth of planted Chir pine (Rauntiainen, 1992), height-diameter relationship (Sharma, 2009; Thapa et al., 2013), basal area growth (Gyawali et al., 2015), growth performance to climate (Sigdel et al., 2018; Tiwari et al., 2020), and allometric volume models (Aryal et al., 2023). Though some stand and individual tree growth models for the species have been developed, none of the studies has focused on developing stem taper function to help improve the upper stem diameter prediction and volume prediction of Chir pine. To ensure sustainable resin tapping and meet timber demand, an approach of scientific forest management requires species-specific individual tree or stand-level growth models. Therefore, this study aims to evaluate the multiple forms of taper equations by improving the residual errors and to provide the best function to describe stem tapering in individual trees of Chir pine. The results from this study are expected to be helpful in estimating upper stem diameter, current and future volume (total and merchantable) and biomass.

2. Materials and methods

2.1. Study area

The study site represents the western hilly region of Nepal. The data were collected from three Chir pine-dominated natural stands managed by the local community as community forests (CFs) in the Palpa district (Fig. 1). Our study sites were Rampokhari CF, Nayadevi CF, and Pakhure CF. In these CFs, the dominant tree species is Chir pine (*Pinus roxburghii*), and other associated species are *Schima wallichii, Shorea robusta, Rhodendron spp.,* and *Castanopsis spp*. These CFs are adjacent to each other. and represent a similar elevational range and topography. These forests were selected to represent various tree size classes, stand densities, ages, and site qualities. The elevations of the studied forests range from 960 m to 1606 m above sea level, and the mean, maximum, and minimum average annual temperatures are 19.6°C, 26.3°C, and 12.8°C, respectively. The mean total annual rainfall is 1581.5 mm (DHM, 2017).

2.2. Sampling and measurements

We consulted the Divisional Forest Office (DFO) of Palpa District to help identify the natural stands of Chir pine that could represent the different development stages (tree, pole, and sapling). Additionally, the CF management plan provided by the community forest user groups helped identify the variation in tree size within and between each forest (Table 1). These three CFs were randomly chosen from a subset of all CFs approved by the DFO for destructive sampling and measurements in the context of ongoing tree felling as a part of forest improvement or tending operation. Considering the different developmental stages and geographical locations, we used a stratified random sampling technique to establish 31 sample plots of 400 m^2 in area (20 m x 20 m). These sample plots were enough to represent the variations in stand conditions, such as D *(cm)*, H *(m)*, stand densities (trees ha^{-1}), and basal area (m^2 ha^{-1}). The summary statistics of the Chir pine forests of these CFs are shown in Table 1. Overall, the stand averages of D, H, basal area, and density were 19.94 cm, 11.45 m, 21.20 m^2 ha^{-1}, and 525 trees ha^{-1}, respectively (Table 1).

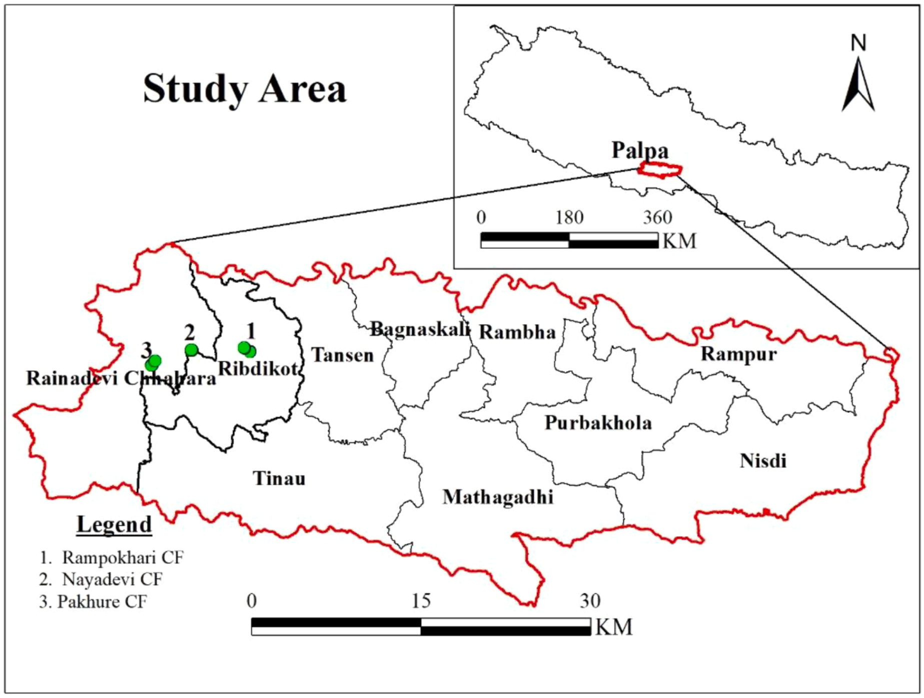

Fig. 1. Location of the study area showing three Chir pine dominant community forests (CFs) in Palpa district, Nepal, where 31 sample plots were established, and destructive sampling and measurement were carried out.

Table 1
Summary statistics (mean ± standard deviation, minimum and maximum) of the individual tree and stand-level attributes of natural Chir pine dominant community forests of the study sites.

Community Forest	Statistics	Tree attributes		Stand attributes	
		D (cm)	*H* (m)	Basal area (m^2ha^{-1})	Density (trees ha^{-1})
Nayadevi	Mean ± Std dev Min, Max	22.97 ± 6.41 10.50, 39.30	14.92 ± 3.58 6.30, 25.30	27.15 ± 2.81 23.24, 31.73	608 ± 63 525, 700
Rampokhari	Mean ± Std dev Min, Max	18.74 ± 12.27 5.80, 79.20	11.70 ± 5.0 5.0, 32.50	22.01 ± 3.69 18.05, 31.52	559 ± 167 300, 875
Pakure	Mean ± Std dev Min, Max	19.37 ± 11.01 5.60, 52.50	9.25 ± 5.39 2.80 ± 27.10	18.02 ± 7.45 11.25, 39.28	463 ± 193 125, 800
Overall	Mean ± Std dev Min, Max	19.94 ± 10.80 5.60, 79.20	11.45 ± 5.34 2.80, 32.50	21.20 ± 6.48 11.25, 39.28	525 ± 173 125, 800

D = diameter at breast height; *H* = total tree height.

2.3. Destructive sampling measurements

We selected healthy and undamaged trees with different size characteristics to represent each stand development stage. Eighty trees (1 to 4 trees from each sample plot) were felled as as part of regular harvesting and thinning activities following CF's management plan. Selected Chir pine harvesting and measurement data were collected between March and June 2022. The *D* of the selected tree ranges from 5.6 to 79.2 cm, and *H* ranges from 3.10 to 32.5 m. The descriptive statistics of all the destructively harvested sample trees are presented in Table 2.

Before felling a tree, diameters were measured at 0.3 m, 0.8 m, and 1.3 m height above the ground using diameter tape to the nearest 0.1 cm. Once the tree felled, the *d* was measured at 2 m, linearly extending from the large butt end of the stem, and subseqenlty at intervals of 1.5 m along the tree stem . Depending upon the total length of a stem, the last measurement interval (*h*) varied for the corresponding *d*. In addition, when branches or any other irregularity occurred at the specified measurement point along the stem, the diameter measurement was taken immediately above the irregularity. The existing range of *D* and *H* and the relative range of *d/D* and *h/H* are shown in Fig. 2 based on destructive sampling.

Table 2
Summary statistics (mean ± standard deviation, minimum and maximum) of the destructively harvested sample trees according to diameter classes. *D*: diameter at breast height (cm); *H*= total length of the stem (m), *n*: number of sample trees.

D class (cm)	*n*	*D* (cm)		*H* (m)	
		Mean ± Std dev	Min, Max	Mean ± Std dev	Min, Max
0-10	10	7.30±1.48	5.60,9.50	4.19±0.87	3.10, 5.30
10-20	14	16.08 ± 2.60	11.90,19.40	9.66±3.00	4.20, 14.60
20-30	8	24.78 ± 2.73	20.50,28.20	16.39 ± 3.40	10.90, 19.80
30-40	17	36.38±2.17	31.80,39.50	19.24±2.61	12.50, 23.20
40-50	22	44.63 ± 2.87	40.10,49.60	22.60±2.42	17.30, 27.10
50-60	5	51.80 ± 0.64	50.80,52.50	24.16 ± 2.97	20.70, 27.10
60-70	2	68.75 ± 0.49	68.40,69.10	31.70 ± 1.13	30.90, 32.50
70-80	2	75.35 ± 5.44	71.50,79.20	31.05 ± 0.92	30.40, 31.70
Overall	80	33.05±16.94	5.6, 79.2	17.24±7.74	3.10, 32.5

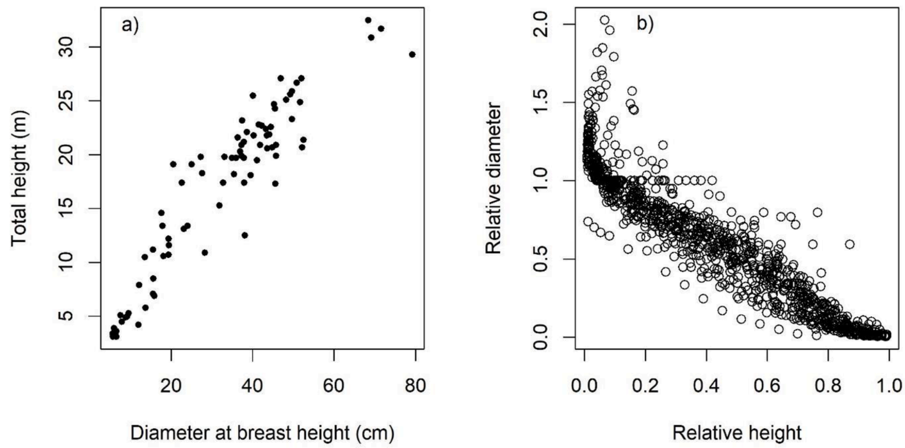

Fig. 2. Scatter plot of total height and diameter at breast height (a) and the relative height plotted against relative diameter (b).

2.4. Taper equations

We selected thirteen commonly used and well-behaved taper equations to fit our data (Table 3) based on the model suggested by (Rojo et al., 2005, Diéguez-Aranda et al., 2006; Li and Weisktittle, 2010; Ulak et al., 2022). Among the included models for comparison, nine models (M1-M9) were single taper form (Kozak et al., 1969; Bennett and Swindel, 1972; Damerschalk, 1972; Omerod, 1973; Clutter, 1980; Amidon, 1984; Pain and Boyer, 1996; Ounwkham, 2009), three models (M10-12) were variable-exponent form (Sharma and Oderwald, 2001; Sharma and Zhang, 2004; Sharma and Parton, 2009) and one model (M13) was segmented form (Max and Burkhart, 1976). Although most of the model forms were developed to predict the ratio d/D, we transformed the equations to predict d.

2.5. Model fitting

Thirteen commonly used taper functions were fitted to our data and evaluated for their performance.We used a nonlinear mixed-effects modeling approach to account for the correlation of the diameter

Table 3
Different forms of taper equations used in the study, M1- M9 are single taper equations, the M10-12 variable-exponent, and the M13 is the segmented form.

Model	Equations	References
M1	$d = D\left\{\beta_0 + \beta_1\left(\frac{h}{H}\right) + \beta_2\left(\frac{h}{H}\right)^2 + \beta_3\left(\frac{h}{H}\right)^3 + \beta_4\left(\frac{h}{H}\right)^4\right\} + \varepsilon_{ij}$	Ounekham (2009)
M2	$d = \beta_0\left\{\frac{D(H-h)}{H-1.3}\right\} + \beta_1(H-h)(h-1.3) + \beta_2 H(H-h)(h-1.3) + \beta_3(H-h)(h-1.3)(H+h+1.3) + \varepsilon_{ij}$	Bennett and Swindel (1972)
M3	$d = \beta_0\left\{\frac{D(H-h)}{H-1.3}\right\} + \beta_1\left\{\frac{\left(H^2-h^2\right)(h-1.3)}{H^2}\right\} + \varepsilon_{ij}$	Amidon (1984)
M4	$d = \sqrt{D^{\beta_0} \times \left(\frac{H-h}{H-1.3}\right)^{\beta_1}} + \varepsilon_{ij}$	Ormerod (1973)
M5	$d = 10^{\beta_0} D^{\beta_1} H^{\beta_2} (H-h)^{\beta_3} + \varepsilon_{ij}$	Demaerschalk (1972)
M6	$d = \beta_0 D^{\beta_1} H^{\beta_2} (H-h)^{\beta_3} + \varepsilon_{ij}$	Clutter (1980)
M7	$d = \sqrt{D^2 \times \left\{\beta_0\left(\frac{h}{H}-1\right) + \beta_1\left(\frac{h^2}{H^2}-1\right)\right\}} + \varepsilon_{ij}$	Kozak et al. (1969)
M8	$d = \beta_0\left\{1 - \left(\frac{h}{H}\right)^3\right\} + \beta_1 \ln\left(\frac{h}{H}\right) + \varepsilon_{ij}$	Pain and Boyer (1996)
M9	$d = D\left(\frac{H-h}{H-1.3}\right)^{\beta_0} + \varepsilon_{ij},\ \beta_0 > 0$	Ormerod (1973)
M10	$d = \sqrt{\beta_0 \times D^2 \times \left[\frac{h}{1.3}\right]^{2-\left\{\beta_1+\beta_2 * \frac{h}{H} + \beta_3\left(\frac{h}{H}\right)^2\right\}} \times \frac{H-h}{H-1.3}} + \varepsilon_{ij}$	Sharma and Zhang (2004)
M11	$d = D\left\{\beta_0\left(\frac{H-h}{H-1.3}\right)\left(\frac{H}{1.3}\right)^{\beta_1+\beta_2\frac{h}{H} + \beta_3\left(\frac{h}{H}\right)^2}\right\}$	Sharma and Parton (2009)
M12	$d = \sqrt{D^2\left(\frac{h}{1.3}\right)^{(2-\beta_0)} \times \left(\frac{H-h}{H-1.3}\right)} + \varepsilon_{ij}$	Sharma and Oderwald (2001)
M13	$d = D\sqrt{\beta_1\left(\frac{h}{H}-1\right) + \beta_2\left(\left(\frac{h}{H}\right)^2 - 1\right) + \beta_3\left(\alpha_1 - \frac{h}{H}\right)^2 I_1 + \beta_3\left(\alpha_4 - \frac{h}{H}\right)^2 I_2}$ $I_1 = 1\ if \frac{h}{H} \leq \alpha_1; otherwwise\ 0; I_2 = 1\ if \frac{h}{H} \leq \alpha_2; otherwwise\ 0$	Max and Brukhart (1976)

Note: D = diameter at breast height; H = total height; d = upper stem diameter at height h; h = height of tree from ground where the d is measured; and $\beta_0, \beta_1, \beta_2, \beta_3, \beta_4$ are the parameters to be estimated.

measured at different heights of the same tree. In this modeling approach, *D, H*, and *h* were considered the fixed effect parameters, and the individual-tree variation was considered as random effects. A random effect of an individual tree was modeled on all individual parameters of models to obtain a better model fit. The model fit with the lowest Akaike Information Criterion (AIC) value for a parameter association of the random effect was selected for further modeling of errors using autocorrelation structure and variance function.Values of all the parameters and fit statistics were estimated using the nlme package (Pinheiro et al., 2018) in Rversion 4.0.5 (R Core Team, 2021). The parameters of the model fitting convergence were reported.

The structure of a general nonlinear mixed-effects model with constant variance is as follows:

$$y_{ij} = f(\phi_{ij}, \upsilon_{ij}) + \varepsilon_{ij} \tag{1}$$

where,

- $i = 1.....k$ is the number of individual trees;
- $j = 1. ......, n$ is the number of upper stem diameter measurements for the i[th] tree;
- ϕ_{ij} is modeled as a non-linear mixed-effects model $\phi_{ij} = \boldsymbol{A}_{ij}\beta + \boldsymbol{B}_i\boldsymbol{b}_i$, where $\boldsymbol{A}_{ij}$ is an individual-specific design matrix for combining fixed effects; $\boldsymbol{B}_i$ is an individual-specific;design matrix for combining random effects;
- υ_{ij} is the vector of covariates in the model;
- $\boldsymbol{b}_i$ is a vector of random effects associated with tree *i* and;
- $\varepsilon_{ij,}$is a vector of random errors describing additive noise.

Since upper stem diameters were measured at different height intervals along the stem, autocorrelation may exist between *d* measurements and non-constant error variance due to stem diameter size at the breast height. Such autocorrelation and heteroscedasticity of variance structure could affect model prediction, and modeling such error structures reduces the predicted mean square errors of a model within a mixed-effect modelling framework (Valentine and Gregoire, 2001; Trincado and Burkhart, 2006; Li and Weiskittel, 2010; Saud et al. 2016; Saud et al., 2019). Therefore, we fitted the nonlinear mixed effect model with the first order of continuous autoregressive correlation structure (corCAR1) and power variance (Pinheiro and Bates, 2000; Cryer and Chan, 2008). We used the likelihood ratio to evaluate the statistical significance of corCAR1 and variance structure, assuming the nested model structure (Pinheiro and Bates, 2000).

The corCAR1 structure was selected because it assumes the autocorrelated errors decrease with time and allows to model autocorrelation for unequally spaced time covariates (Arias-Rodil et al., 2015; Adamec et al., 2019). The construction of taper equation requires the measurements of *d* at different *h* along the stem for each tree. These multiple observations within each tree are spatially correlated and form longitudinal data structure, violating the assumption of independent errors (Rojo et al., 2005; Diéguez-Aranda et al., 2006; Yang et al., 2009). While measuring *d* along the stem, the selection of *h* points is often unequally spaced, which is equivalent to measurements taken at different time points in a time series, thus introducing inherent autocorrelation in the longitudinal data. However due to the difference in total height between trees and the exclusion of branches location along the stem, the measurements points could be irregular and unbalanced, which are typical characteristic of forestry data. Thus corCAR1, which models continuous-time autoregressive structure and does not requires equally spaced time intervals, was selected to address the autocorrelation of the measurements.

Trees grown in high density have a lower taper ratio than those grown in low-density or open space. Therefore, we assumed that *D* of a tree regulates variability in the upper stem diameter (*d*) and taperness. Although relative height (Tricando and Burkhart, 2006; Li and Weiskittel, 2010) and relative height and diameter (Valentine and Gregoire, 2001; Li and Weiskittel, 2010) can be considered as power variance, we selected only the weight of *D* as the power variance function to model the heterogeneity in residuals (Saud et al., 2016; Saud et al., 2019).

The structure of corCAR1 and the power variance function is shown below. corCAR1 models the correlated errors *(ε_{it}) as*:

$$\varepsilon_{ij} = \phi_1 \varepsilon_{ih-1} + \omega_{ih} \tag{2}$$

where ω is an additional error and $\omega_{it} \sim iid\ N(0, \sigma_w^2)$,

i is the individual tree, *h* is the measurement point (lag), and φ is the autocorrelation between lags. The correlation "rho" (ρ) between residuals of an observation pair declines exponentially with the number of *d* measured at *h* apart, i.e., $\rho = \phi_{.}^{h}$

Power variance function

$$var(\varepsilon_{ij}) = \sigma^2 |v_{ij}|^{2\delta} \tag{3}$$

Error variance (ε_{ij}) was modeled, where υ_{ij} is the *D* covariate and δ is the power parameter. The variance function assumes heterogeneity with in-tree variance as a function of *D*.

2.6. Model evaluation

The competing equation form for the best parameter association with the random effect within a model were evaluated using the likelihood ratio test (χ^2). The model which produces the lowest AIC value when fitted with the first order of corCAR1 and power variance was selected as better fit model. A model-equation form with only random effects and with modeling of error structures were also compared using the likelihood ratio test. We conducted k-fold cross-validation for the mixed-effect models with error structures. Considering the sample size, we chose k =5 folds to ensure that the model does not suffer from high variance and high bias. This approach uses k-1 folds to fit the data and remaining fold as validation set, which is equivalent to an 80/20% split of the whole data. The fitted taper functions were evaluated using different criteria, including the significance of estimated parameters (at a 5% level of significance); fit index (*FI*) as the coefficient of determination (pseudo-R^2) (higher values indicate better models) (Eq. 4); root mean squared error (*RMSE*; lower values indicate better models) (Eq. 5) (Montgomery et al., 2001); and *AIC* (lower values indicate better models) (Eq. 6) (Akaike, 1974; Burnham and Anderson, 2002); mean absolute error (*MAE;* lower the value, better a model fit) (Eq. 7). The *FI* is also called pseudo-R^2, which measures the goodness of fit of the nonlinear model (Saud et al., 2016). The distribution of residuals was plotted against the predicted upper stem diameter to evaluate whether the taper function had asystematic bias. Residuals were also plotted against the predictor variables and examined for evidence of bias. The best taper functions within and between the three different from were selected using the above evaluation criteria.

$$FI = 1 - \frac{\sum_{i=1}^{n}(y_i - \hat{y}_i)^2}{\sum_{i=1}^{n}(y_i - \bar{y}_i)^2} \tag{4}$$

$$RMSE = \sqrt{\frac{\sum_{i=1}^{n}(y_i - \hat{y}_i)^2}{n}} \tag{5}$$

$$AIC = -2\ln(L) + 2p \tag{6}$$

$$MAE = \frac{\sum_{i=1}^{n}|y_i - \hat{y}_i|}{n} \tag{7}$$

where y_i = observed *d*,$\hat{y}_i$= predicted *d*, $\bar{y}_i$= mean of *d*, *L* = maximum likilhood function, and *p* = number of parameters. The model with the lowest values for the goodness of fit was considered the best.

3. Results

Mixed-effects model fitted with the random effect associated with the individual tree for taper equations showed reduced AIC values at different parameters within a model (Table 4). A likelihood ratio, the goodness of model fit, indicated that the location of parameters significantly differs with random effects association. A significant reduction in the model AIC value was found in the models; M1-M4, M7, M8, M10, M11, and M13. The model with a lower AIC value was due to the significant association of random effect at different parameter locations ($p < 0.001$). However, the likelihood ratio test values were not significantly different among the parameters of the model when AIC values were similar, such as M2 (β_1 and β_2), M5 (β_1, β_2, and β_3), M6 (β_1, β_2, and β_3).

3.1. Taper equation and performance

All selected models with random effects associated with different parameters were fitted with the corCAR1 structure and power variance function. The parameter estimates and fit statistics (*FI, RMSE, MAE*, and *AIC*) for the taper functions evaluated in this study are presented in Table 5. The parameter estimates of all models were significantly different and described a variation of more than 95% in predicting *d* at the specific height of a stem (Tables 5 & 6). The models fitted with only the random effect associated with the individual tree showed better variability (*FI*) and smaller error (*RMSE, MAE*) than those fitted with corCAR1 and power variance. As expected, the likelihood test of all models fitted with corAR1 and power variance significantly differed from the random effect model. This improvement was due to adding parameters in a nested structure to a model that further showed an increase in the positive coefficient and a decrease in the negative coefficient. All equations fitted with corCAR1 and power variance showed a significant reduction in the variability due to the random effect of an individual tree in predicting upper stem diameter.

Among the single taper function, M2 and M3 showed better-fit statistics accounting for the amount of error due to autocorrelation and variance structure than other compared models (Table 5), as well in the k-fold cross validation (Table 7). Other models, such as M7, M8, and M9, showed strong autocorrelation ($\phi > 0.87$) and a higher amount of variance weight (M7; $var(\varepsilon_{ij}) = 0.41$) in the error structure of those models resulting in increased *RMSE* and *MAE* value. Similarly, among the variable-exponent model form, M10 showed better-fit statistics with comparable M11 (Table 5 & 7). However, the M12 showed more error in prediction due to high autocorrelation ($\phi = 0.89$) and power variance ($var(\varepsilon_{ij}) = 0.43$). The segmented model form (M13) also showed improved parameter estimates but indicated high autocorrelation of the error structure (Table 6). Overall, the M10, the variable-exponent model form, was a better taper equation with higher *FI*, lower *RMSE, MAE,* and *AIC* value than the competing single taper form (M2, M3) and a segmented model (M13) even in k-fold crossvalidation (Table 7).

Table 4
Akaike Information Criteria (AIC) value of taper equation forms fitted with a single random effect (σ_k) associated with the different positions of parameters (*β*) within a model.

Equation form	Model	AIC value				
		$\sigma_k\beta_0$	$\sigma_k\beta_1$	$\sigma_k\beta_2$	$\sigma_k\beta_3$	$\sigma_k\beta_4$
Single	M1	4890*	4931	5233	5403	5496
Single	M2	5120	4657*	4659	4595	-
Single	M3	5327	4596*	-	-	-
Single	M4	5293	4822*	-	-	-
Single	M5	5292	5287	5286*	5352	-
Single	M6	5296	5287	5286*	5351	-
Single	M7	6063	5431*	-	-	-
Single	M8	5908*	6829	-	-	-
Single	M9	4914	-	-	-	-
Variable	M10	5126	4889	4380*	4600	-
Variable	M11	5345	5336	4559*	4615	-
Variable	M12	5461	-	-	-	-
Segmented	M13	-	4987	4776*	5488	5575

* Random effects associated with a parameter were significantly different in the likelihood ratio test within a model, except for the M2, M5, and M6, where the AIC value was similar.

3.2. Residual diagnostic

The residual analysis of the selected model showed similar trends with a slight difference in the variability with the increasing fitted values (Fig. 3). The M2, M3, and M10 showed higher standardized residual values. In contrast, the M13 did not show such pattern but more funneling toward the higher fitted values. Further, plotting the residuals against the *h* suggested the segmented equation, M13, had higher errors in *d* than other models (Fig. 4). The variable-exponent model (M10) showed a more condensed prediction error centering the zero than the single taper equation along 8-20 m stem length. This result suggests that other models would produce high errors in estimating volume when these models are used to predict upper stem diameter. This diagnostic analysis of residuals indicated that the M10 is the best among the competing models, M2, M3, and M13.

4. Discussions

This study is the first to offer a different form of taper equation for the natural forest stand of Chir pine distribution in the Himalayan region, including Nepal, India, Pakistan, and Bhutan. Three different forms of taper equations fitted with nonlinear mixed-effects modeling approaches were found well fit to predict the upper stem diameters of an individual tree of a natural stand of Chir pine. The single taper equation form performed better than other forms, as further confirmed by k-fold cross validation procedure. We found that the variability in predicting upper stem diameter was inconsistent along the length of a stem, which would eventually influence the volume or biomass estimation for accounting potential carbon sequestration in the region. Along the Chir Pine distributional range, studies that either use or develop allometric equations for estimating volume or biomass suggest that tree height exhibits higher variability in predicting total volume or biomass compared to diameter. For example, allometric equations using diameter at breast height have been reported as strong predictors for explaining higher variability in Pakistan (Khan et al., 2014; Ali et al., 2020), India (Jain et al., 2021), and Nepal (Aryal et al., 2023). However, adding total height to the model only marginally improved performance due to the higher variability in height measurements. Tenzin (2017) developed a form factor for Chir pine in Bhutan also indicated that diameter and height explained only 43% variability in characterizing the shape of a tree. Indeed, the height growth of Chir Pine, influenced by density, altitudinal variation, and climate along the distributional range, affects estimating total productivity, which significantly contributes to variation in biomass and carbon estimation (Rana et al., 1989; Sigdel et al., 2018; Tiwari et al., 2020; Kumar et al., 2021).

Unlike the plantation stand of other pine species around the world, variability in the natural stand of Chir pine showed a large magnitude of *RMSE* > 1.5 cm, although the *FI* was more than 95% in all models. Similar to our result, Li and Wieskittel (2010) reported *RMSE* of 1.6 to 2.2 cm when comparing multiple taper equations for the natural stand of White pine (*Pinus strobus* L.) in the Acadian Region of Canada. Tricando and Burkhart (2006) also reported the lowest precision for the taper equation in the natural stand of Loblolly pine (*Pinus Taeda* L.) compared to intensively managed loblolly pine plantations in the USA. Because of differences in the stand density, age, and site, the size and height of a tree would exhibit huge variation, offering different stem shapes compared to plantation stand. However, the model fitted to the plantation pines species has a reasonably lower value of error than natural

Table 5
Parameter estimates and fit statistics of the single (M1-M9) and variable-exponent taper function models (M10-M12) fitted with random effect (σ_k) and including modeling error structure of corCAR1 (ϕ) and power variance ($var(\varepsilon_{ij})$).

Model	Parameter estimates					Errors				Fit statistics			
	β_0	β_1	β_2	β_3	β_4	ε_{ij}	$\sigma_{k\beta}$	ϕ	$var(\varepsilon_{ij})$	*FI*	*RMSE*	*MAE*	*AIC*
M1	1.138	-1.870	5.045	-7.804	3.595	2.152	0.056 $_{b0}$	-	-	0.982	2.104	1.600	4890
	1.154	-2.384	7.015	-10.425	4.719	0.936	0.035 $_{b0}$	0.867	0.295	0.972	2.621	1.912	3927*
M2	1.019	0.071	-0.004	0.003	-	1.864	0.001 $_{b3}$	-	-	0.986	1.820	1.321	4595
	1.044	0.100	-0.008	0.004	-	0.978	0.001 $_{b3}$	0.751	0.228	**0.982**	**2.070**	**1.528**	**4106***
M3	1.012	0.931	-	-	-	1.874	0.479 $_{b1}$	-	-	0.986	1.822	1.323	4596
	1.037	0.778	-	-	-	0.842	0.434 $_{b1}$	0.740	0.271	**0.983**	**2.007**	**1.531**	**4149***
M4	2.013	1.347	-	-	-	2.088	0.327 $_{b1}$	-	-	0.983	2.029	1.470	4822
	2.025	1.429	-	-	-	0.715	0.251 $_{b1}$	0.787	0.345	0.977	2.342	1.756	4182*
M5	0.201	0.979	-0.803	0.702	-	2.692	0.013 $_{b1}$	-	-	0.971	2.636	2.000	5287
	0.192	0.972	-0.821	0.743	-	0.812	<0.000 $_{b1}$	0.851	0.360	0.958	3.197	2.342	4197*
M6	1.590	0.979	-0.803	0.702	-	2.692	0.013 $_{b1}$	-	-	0.971	2.634	2.001	5287
	1.557	0.972	-0.821	0.743	-	0.813	<0.000 $_{b1}$	0.851	0.359	0.958	3.196	2.342	4198*
M7	-1.806	876.3	-	-	-	2.393	912.1 $_{b1}$	-	-	0.978	2.304	1.774	5431
	-1.150	4.883	-	-	-	1.042	0.008 $_{b1}$	0.928	0.411	0.886	5.247	3.482	4457*
M8	22.836	-4.089	-	-	-	3.123	13.587 $_{b0}$	-	-	0.963	3.010	2.156	5908
	24.279	-2.655	-	-	-	1.741	14.207 $_{b0}$	0.951	0.268	0.943	3.704	2.497	4339*
M9	0.649	-	-	-	-	2.192	0.158 $_{b0}$	-	-	0.981	2.131	1.504	4914
	0.725	-	-	-	-	0.931	<0.000 $_{b0}$	0.870	0.344	0.955	3.314	2.368	4240*
M10	0.989	2.131	0.721	-1.054	1.679$_{b2}$	0.229 $_{b2}$	-	-	0.989	1.634	1.147	4380	M10
	0.989	2.124	0.710	-1.059	0.596$_{b2}$	0.203 $_{b2}$	0.753	0.322	**0.988**	**1.702**	**1.202**	**3769***	
M11	0.907	0.035	0.115	0.159	1.825$_{b2}$	0.095 $_{b2}$	-	-	0.987	1.775	1.319	4559	M11
	0.946	0.034	0.145	0.256	0.861	0.081 $_{b2}$	0.741	0.258	0.983	1.981	1.519	4104	
M12	2.088	-	-	-	2.921$_{b0}$	0.076 $_{b0}$	-	-	0.966	2.854	1.934	5461	M12
	2.108	-	-	-	0.680$_{b0}$	0.029 $_{b0}$	0.897	0.432	0.950	3.501	2.408	4056	

* Likliehood ratio test significance for the model fitted with corCAR1 and power variance than a model with only a random effect model. Subscript b with a number indicates the parameter in the model associated with the random effect.

Table 6
Parameter estimate of the Max and Burkhart (1976) segmented taper function fitted as mixed-effects model and with corCAR1 and power variance structure.

Parameters	Mixed-effects Coefficients	corCAR1 and variance Coefficients
β_1	-3.566	-4.085
β_2	1.621	1.955
β_3	-1.724	-2.014
β_4	43.16	46.417
α_1	0.703	0.729
α_2	0.081	0.081
ε_{ij}	2.048	1.105
σ_k	0.102	0.073
Φ	-	0.870
$var(\varepsilon_{ij})$	-	0.240
AIC	4776	3866*
FI	0.98	0.975
RMSE	2.00	2.470
MAE	1.536	1.808

Table 7
Model fit statistics (*RMSE, MAE and FI*) of the taper equation forms based on the k= 5-fold cross-validation of the mixed-effect model with error structure.

Equation form	Model	Fit statistics		
		RMSE	*MAE*	*FI*
Single	M1	2.5106	1.8809	0.9731
Single	M2	**2.0004**	**1.5289**	**0.9827**
Single	M3	**2.0165**	**1.5638**	**0.9829**
Single	M4	2.3441	1.7767	0.9765
Single	M5	3.1078	2.2956	0.9587
Single	M6	3.1080	2.2958	0.9587
Single	M7	5.0904	3.4646	0.8901
Single	M8	3.4772	2.4222	0.9494
Single	M9	3.2698	2.3532	0.9552
Variable	M10	**1.7261**	**1.2337**	**0.9873**
Variable	M11	1.9884	1.5424	0.9832
Variable	M12	3.4167	2.3878	0.9501
Segmented	M13	2.3155	1.7552	0.9774

stands, such as Loblolly pine in the USA (Cao, 2009; Sabatia and Burkhart, 2015; Lynch et al., 2017); Radiata pine (*Pinus radiata* D. Don) in New Zealand (Goulding and Murray, 1976; Sabatia and Burkhart, 2015), Spain (Arias-Rodil et al., 2015), Australia (Bi and Yong, 2001), Jack pine (*Pinus mariana* Lamb.) in Canada (Sharma and Patron, 2004); Scot pine (*Pinus sylvestris* L.) in Turkey (Özçelik and Brooks, 2012).

Mixed-effects modeling with the autocorrelation and variance structure provided improved parameter estimates and a smaller error (ε_{ij}) error than the mixed-effects model without error structure (Table 5). As expected, the variability in prediction error contributed to the structure of residual errors associated with the random effect of an individual tree. Studies on taper equations have shown a better model performance when more than two parameters are considered for random effects (Trincando and Burkhart, 2006; Sabatia and Burkhart, 2015; Arias-Rodil et al., 2015). Considering more than two random effects in the model introduces the between-tree variations (Arias-Rodil et al., 2015); however, in the destructive sampling, only one or two sample trees are harvested from different plots, and all samples do not belong to the same plot. In such a case, the between-tree variation does not exist because the plot-level random effect associated with the selected tree for harvesting is equivalent to the between-tree variation for that stand. Instead of inclusion of this between-tree variation and overparameterization of a mixed-effects model, we also fitted the nested random effect of the site on an individual tree that did not show any difference in the coefficient estimates and error with just a single parameter of random effect. In such case, the mixed-effects model indicated that the variation between trees due to the plot (Eqs. 2, 5, 6, 7, & 9) could be minimized $(\sigma_k < 0.01)$ because of high autocorrelation$(\phi > 0.80)$ and variability from the D $(var(\varepsilon_{ij}) > 0.24)$ that influence the prediction of d.

The residual distribution of the selected model along the relative height was similar in pattern to Trincado and Burkhat (2006) fitted to loblolly pine. The increasing error for d with the relative height could produce a negative bias in the volume estimation (Arias-Rodil et al., 2015). Nevertheless, the performance of a taper equation could vary between species, and the choice of equation form selected to fit a species

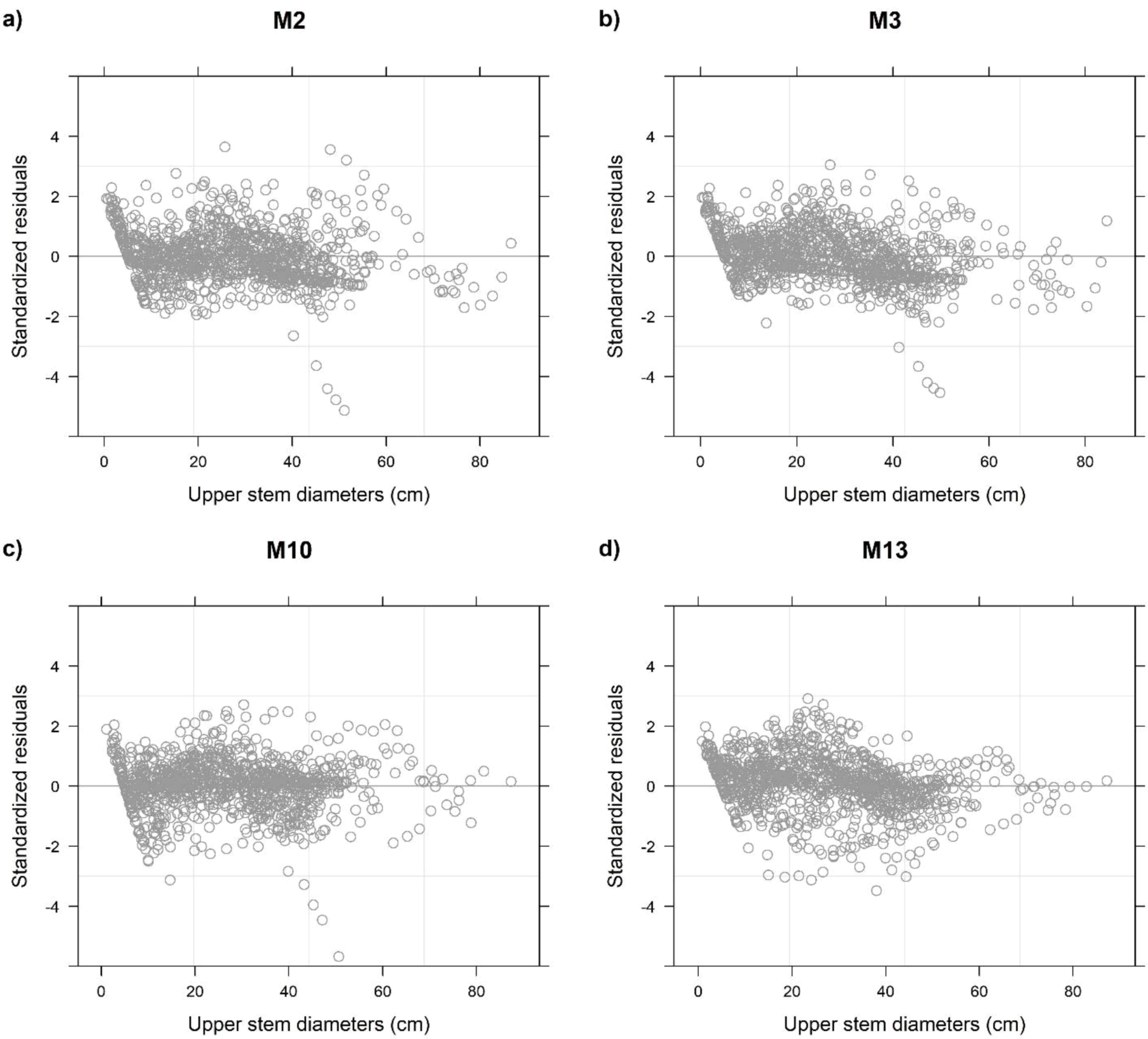

Fig. 3. Standardized residual against the fitted value of the selected taper equations model. The single taper equations (a & b, M2 and M3), variable-exponent (c, M10), and the segmented equation (d, M13).

may show a high or low error in predicting *d* along the length of a stem. For example, Sharma and Oderwald (2001) fitted Eq.(12) and Eq.(13) to the natural stand of loblolly pine grown in North Carolina, USA. Their study demonstrated a similar pattern in estimating the bias and precision with increasing relative height (h/H), as observed in the Fig. (3) for Eq.(10) and Eq.(13). Likewise, Sharma and Zang (2004) also found that Eq.(10) had a smaller error than the Eq.(13) fitted to the planted Jack pine (*Pinus banksiana* Lamb) in Canada. Because of such variability, a model fit error is often compared at the percentage of a relative height (Max and Burkhart, 1976; Arias-Rodil et al., 2015; Zhao et al., 2019).

The performance of the variable-exponent form was found to be better than the segmented model because the parameter estimates of β_0 largely regulates the butt diameter and depends on the *D* of an individual tree. The estimate of β_0 describes the shape of the conifer tree. In the segmented equation, the points of inflection (α_1, α_2) regulate the prediction of*d* at varying *h* along the stem. Because of this, the segmented equation could provide a smaller error depending on therange in the *D* and *H* of a species (Cao, 2009; Sabita and Burkhart, 2015; Lynch et al., 2017) when the Eq.(13) fitted to relatively smaller ranges of *D* and *H* than our dataset. Sabaita and Burkhart (2015) found that Eq. (13) produced *RMSE* of 1.3 cm for Loblloy pine while it was of 4.29 cm for Radiata pine, where the maximum value of *D* and *H* of Radiata pine was two times that of Loblolly pine. It helped us to conclude that Eq.(13) might not perform better for fitting taller trees, as we noticed in our study. It is also further supported by the work of Sharma and Zhang (2004) for pine and fir species in Canada and Ulak et al. (2022) for *Shorea robusta* in Nepal, where the variable-exponent model performed better than segmented and single-from, respectively, while fitting with the trees of average height greater than 17-19 m, similar to our study. Rojo et al. (2005) also reported a variable-exponent model that performed better than other taper equations for the natural stand of Maritime Pine (*Pinus pinaster*) in Spain. A study by Özçelik and Brooks (2012) also indicated that the fit index was better for the three commercial pines of Turkey fitted with the Clark segmented model (Clark et al., 1991) than Eq.(13), where the average height was greater than 17 m. This Clark model has four segments to combine the butt section, lower stem, middle stem, and upper stem, while Eq.(13) has only two segments. A segmented taper equation with more than two segments would better predict stem diameter (Valenti and Cao, 1986). However, Amidon (1984) reported Eq. (13) had less bias compared to single-variable form (Eqs. 2, 3, 5 & 7) for the natural stand of Ponderosa pine (*Pinus ponderosa* Doug.), but reported Eq.(3) and Eq.(5) has less bias than Eq.(13) for the Sugar pine (*P. lambertiana* Dougl.) trees felled from mixed conifer forest of California, USA. It could be possible because the taper equation was

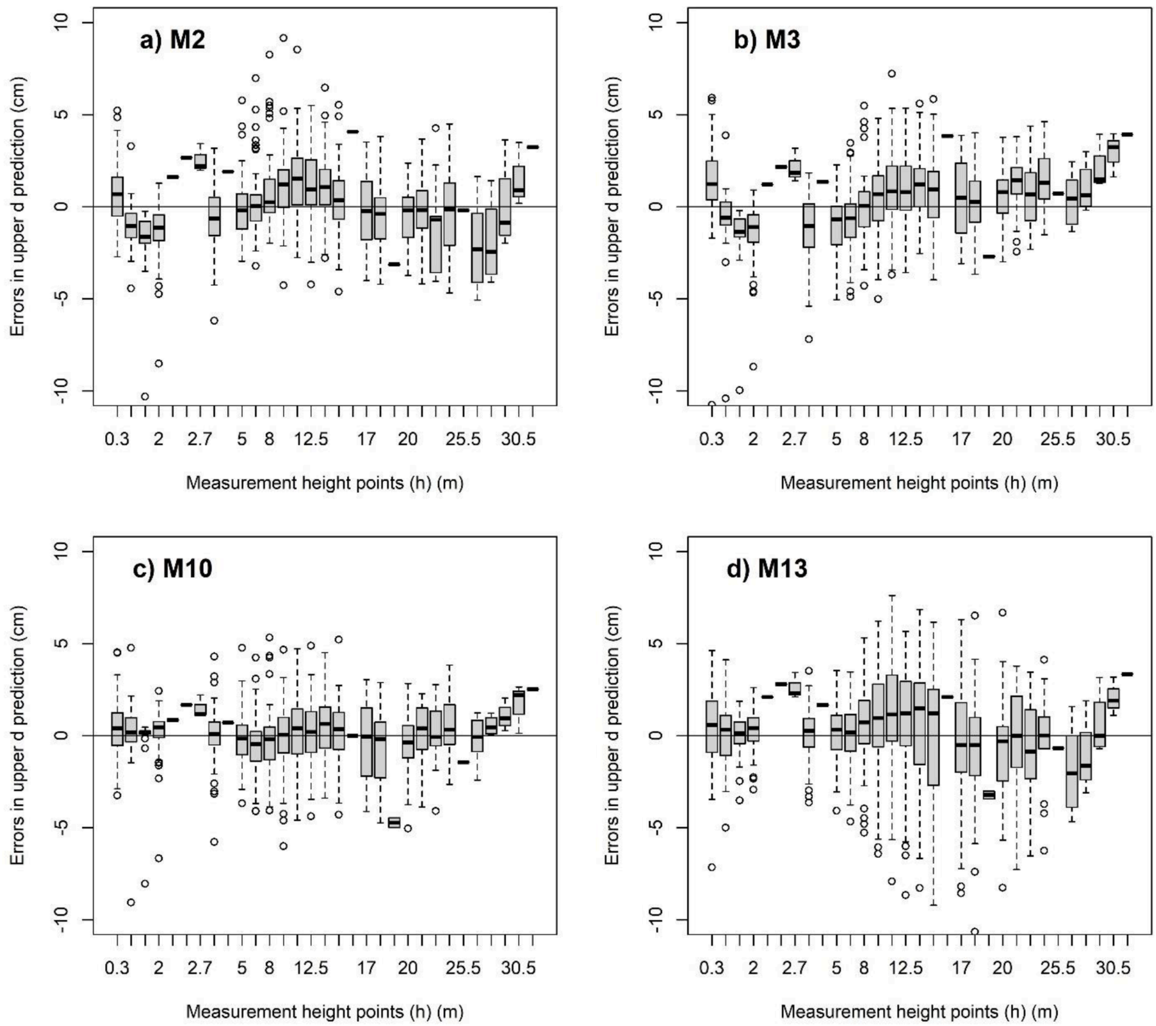

Fig. 4. Boxplots showing the variation in the upper stem diameter prediction (*d*) at different measurement height points (*h*) along the stem. The single taper equations (a &b, M2 and M3), variable-exponent(c, M10), and the segmented equation (d, M13). The box represents the interquartile range, the whisker represents the maximum and minimum error, and the circle represents the outliers.

fitted using the crossectional cuts of the stem, and *D* and *H* range from 15-81 cm and 7-40 m for Ponderosa pine. Indeed, those minimum values were larger than *D* (5.6 – 79.2 cm) and *H* (3.1- 32.5 m) in our data, which indicates a better fit for a merchantable size tree.

Studies showed that the taper equation performed better when the stem diameter was measured inside the bark rather than outside, but the model performance could vary by tree species (Sharma and Patron, 2009; Sharma and Zhang, 2004; Li and Wieskitell, 2010). However, our study includes only the diameter measured outside the bark, which could be a reason for showing a higher *RMSE* value. Further, most of the taper equations were modeled as the ratio of $\frac{d}{D}$ or $\frac{d^2}{D^2}$ which helps yield a marginal reduction in *RMSE* (Sharma and Zhang, 2004) as the right hand of the side of the equation condition the variable in the ratio form. However, the performance of the equations could be improved using the stem density variable (Sharma and Patron, 2009; Ulak et al., 2022) and crown ratio (Valenti and Cao, 1986; Jiang et al., 2007; Li and Weiskittel, 2010). In our study, the variability could be due to some difference in *D* and *H* among the site because of the high stem density; some sites had larger trees than others. In the future, including stem density and crown ratio in the taper equation could help provide a better parameter estimate.

5. Conclusion

In this study, we developed a taper function for one of the most important timber species (Chir pine) in the mid-hills of Nepal, employing the data from 80 individual trees across three forest stands. Thirteen different taper functions of three forms (single, variable-exponent, and segmented) were compared using mixed-effect modeling by selecting the best parameter association with the random effect to avoid overparameterization. Models were further fitted to minimize errors by modeling the variance and the correlation structure and model performances were validated using k-fold cross-validation procedure The taper function of Sharma and Zhang (2004) best predicted diameter at different stem heights among the candidate taper functions. The taper function developed in this study could be useful in predicting upper stem diameters, merchantable volumes, total volume, biomass, and carbon of individual trees in natural forest stands of Chir pine in Nepal.

CRediT authorship contribution statement

Pradip Saud: Writing – review & editing, Writing – original draft, Visualization, Validation, Supervision, Software, Resources, Methodology, Investigation, Funding acquisition, Formal analysis, Conceptualization. **Tolak R. Chapagain:** Writing – review & editing, Resources, Project administration, Data curation, Conceptualization. **Shes K. Bhandari:** Writing – review & editing, Validation, Methodology, Investigation, Formal analysis, Conceptualization. **W. Keith Moser:** Writing – review & editing.

Declaration of competing interest

The authors declare that they have no known competing financial interests or personal relationships that could have appeared to influence the work reported in this paper.

Data availability

Data will be made available on request.

Funding

This research did not receive any specific grant from funding agencies.

Acknowledgements

We would like to thank anonymuous reviwer for their valuable time and constructive feedback,which significantly improved this manuscript. We would like to thank Arkansas Forest Resource Center, College of Forestry, Agricultural & Natural Resources at the University of Arkansas at Monticello, and Arkansas Center for Forest Business for the research support in preparing and publishing this work. We would also thank the USDA Forest Service, Rocky Mountain Research Station, USA for their support in preparing this material. The findings and conclusions in this publication are those of the authors and should not be construed to represent any official USDA or US Government determination or policy. Any use of trade, product, or firm names is for descriptive purposes only and does not imply endorsement by the U.S. Government.

References

Adamec, Z., Adolt, R., Drápela, K., Závodský, J., 2019. Evaluation of different calibration approaches for merchantable volume predictions of Norway spruce using nonlinear mixed effects model. Forests 10 (12), 1104.
Akaike, H, 1974. A new look at statistical model identification. IEEE Trans. Automat. Control 19 (6), 716–723.
Ali, A., Ashraf, M.I., Gulzar, S., Akmal, M., 2020. Development of an allometric model for biomass estimation of Pinus roxburghii, growing in subtropical pine forests of Khyber Pakhtunkhwa, Pakistan. Sarhad J. Agric. 36 (1), 236–244.
Amidon, EL, 1984. A general taper functional form to predict bole volume for five mixed conifer species in California. For. Sci. 30, 166–171.
Arias-Rodil, M, Diéguez-Aranda, U, Burkhart, HE, 2017. Effects of measurement error in total tree height and upper-stem diameter on stem volume prediction. For. Sci. 63 (3), 250–260.
Arias-Rodil, M, Diéguez-Aranda, U, Rodríguez Puerta, F, López-Sánchez, CA, CangaLíbano, E, CámaraObregón, A, Castedo-Dorado, F, 2015. Modelling and localizing a stem taper function for Pinus radiata in Spain. Can. J. For. Res. 45 (6), 647–658.
Aryal, K.R., Chapagain, T.R., Basukala, R.K., Khadka, S., Chaudhary, G., Budha, R.K., Adhikari, H., Khatri, J.R., Sharma, R.P., 2023. Allometric tree volume models for Pinus roxberghii and Cedrus deodara in Karnali Province, Nepal. For. Ecol. Manage 546, 121364.
Behre, E.C., 1923. Preliminary notes on studies of tree form. J. For. 21 (5), 507–511.
Bennett, FA, Swindel, BF, 1972. Taper Curves for Planted Slash Pine. USDA Forest Service Research Note, p. 179.
Bi, H, Long, Y, 2001. Flexible taper equation for site-specific management of *Pinus radiata* in New South Wales, Australia. For. Ecol. Manag. 148 (1-3), 79–91.
Bisht, AS, Singh, S, Kumar, M, 2014. Pine needles a source of energy for Himalayan region. Int. J. Sci. Technol. Res. 3 (12), 161–164.
Burnham, KP, Anderson, DR, 2002. Model Selection and Inference: a Practical Information-Theoretic Approach. Springer-Verlag, New York, USA.
Cao, QV, 2009. Calibrating a segmented taper equation with two diameter measurements. Southern J. Appl. Forest. 33 (2), 58–61.
Cao, QV, Burkhart, HE, Max, TA, 1980. Evaluation of two methods for cubic-volume prediction of loblolly pine to any merchantable limit. For. Sci. 26 (1), 71–80.
Cao, QV, Wang, J, 2011. Calibrating fixed-and mixed-effects taper equations. For. Ecol. Manag. 262 (4), 671–673.
Cao, QV, Wang, J, 2015. Evaluation of methods for calibrating a tree taper equation. For. Sci. 61 (2), 213–219.
Clark III, A, Souter, RA, Schlaegel, BE, 1991. Stem profile equations for southern tree species. US For. Serv. Res. Pap. 113. SE forest experiment station-282.
Clutter, JL, 1980. Development of taper functions from variable-top merchantable volume equations. For. Sci. 26, 117–120.
Cryer, JD, Chan, K-S, 2008. Time Series Analysis: With Applications in R. Springer.
Demaerschalk, JP, 1972. Converting volume equations to compatible taper equations. For. Sci. 18 (3), 241–245.
Demaerschalk, JP, Kozak, A, 1977. The whole-bole system: a conditioned dual-equation system for precise prediction of tree profiles. Canadian J. For. Res. 7 (3), 488–497.
DFRS, 2015. State of Nepal's Forest. Forest Resource Assessment (FRA) Nepal. Department of Forest Research and Survey (DFRS), Kathmandu, Nepal, p. 73.
DHM, 2017. Observed Climate Trend Analysis in the Districts and Physiographic Regions of Nepal (1971-2014). Department of Hydrology and Meterology (DHM), Kathmandu, Nepal (Issue June).
Diéguez-Aranda, U, Castedo-Dorado, F, Álvarez-González, JG, Rojo, A, 2006. Compatible taper function for Scots pine plantations in northwestern Spain. Canadian J. For. Res. 36 (5), 1190–1205.
Fang, Z, Borders, BE, Bailey, RL, 2000. Compatible volume-taper models for loblolly and slash pine based on a system with segmented-stem form factors. For. Sci. 46 (1), 1–12.
Farrar, Robert Jr., M., Jr., Murphy, P.A., 1987. Taper Functions for Predicting Product Volumes in Natural Shortleaf Pines. USDA Forest Service, Southern Research Experiment Station, New Orleans, Lousiana, p. 9. Researh Paper SO-234.
Garber, SM, Maguire, DA, 2003. Modeling stem taper of three central Oregon species using nonlinear mixed effects models and autoregressive error structures. For. Ecol. Manage 179, 507–522.
Gómez-García, E, Crecente-Campo, F, Diéguez-Aranda, U, 2013. Selection of mixed-effects parameters in a variable–exponent taper equation for birch trees in northwestern Spain. Ann. For. Sci. 70, 707–715.
Gordon, AD, 1983. Comparison of compatible polynomial taper equations. N.Z. J. For. Sci. 13, 146–155.
Goulding, CJ, Murray, JC, 1976. Polynomial taper equations that are compatible with tree volume equations. N.Z. J. For. Sci. 5 (3), 313–322.
Gyawali, A, Sharma, RP, Bhandari, SK, 2015. Individual tree basal area growth models for Chir pine (*Pinus roxberghii Sarg.*) in western Nepal. J. For. Sci. 61 (12), 535–543.
Hussain, A, Shahzad, MK, He, P, Jiang, L, 2020. Stem taper equations for three major conifer species of Northeast China. Scand. J. For. Res. 562–576.
Jackson, JK, 1994. Manual of Aforestation in Nepal. Forest Research and Survey Center, Kathmandu, Nepal.
Jain, H., Tyagi, K., Paygude, A., Kumar, P., Singh, R.K., Kumar, M., 2021. Allometric equations for the estimation of biomass and carbon in the sub-tropical pine forests of India. Clim. Impacts Sustain. Nat. Resour. Manage. 89–107.
Jiang, L, Brooks, JR, Hobbs, GR, 2007. Using crown ratio in yellow-poplar compatible taper and volume equations. Northern J. Appl. Forest. 24 (4), 271–275.
Joshi, MR, 1985. Prediction of Biomass in Plantation Stands of Chir pine (*Pinus roxburghii* Sarg.) in Nepal. University of Oxford, UK. MSc thesis.
Joshi, RB, 1984. Total and Merchantable Volume Equations for Natural Silver Fir and Chir pine of Nepal. MSc thesis. University of Athens, Georgia, U.S.A.Kathmandu, Nepal, p. 35.
Khan, N., Ali, K., Shaukat, S., 2014. Phytosociology, structure and dynamics of Pinus roxburghii associations from Northern Pakistan. J. For. Res. 25, 511–521.
Kozak, A, 1988. A variable-exponent taper equation. Can. J. For. Res. 18 (11), 1363–1368. https://doi.org/10.1139/x88-213.
Kozak, A, Munro, DD, Smith, JHG, 1969. Taper functions and their application in forest inventory. Forest. Chronicle 45 (4), 278–283.
Kumar, M., Kumar, A., Kumar, R., Konsam, B., Pala, N.A., Bhat, J.A., 2021. Carbon stock potential in Pinus roxburghii forests of Indian Himalayan regions. Environ. Dev. Sustain. 23, 12463–12478.
Li, R., Weiskittel, AR, 2010. Comparison of model forms for estimating stem taper and volume in the primary conifer species of the North American Acadian Region. Ann. For. Sci. 67 (3), 302. https://doi.org/10.1051/forest/2009109.
Lynch, TB, Zhao, D, Harges, W, McTague, JP, 2017. Deriving compatible taper functions from volume ratio equations based on upper-stem height. Canadian J. For. Res. 47 (10), 1424–1431.
Matte, L, 1949. The taper of coniferous species with special reference to loblolly pine. Forest. Chronicle 25 (1), 21–31.
Max, TA, Burkhart, HE, 1976. Segmented polynomial regression applied to taper equations. For. Sci. 22 (3), 283–289.
Montgomery, DC, Peck, EA, Vining, GG, 2001. Introduction to Linear Regression Analysis. Wiley, New York, USA, p. 641.
Ormerod, DW, 1973. A simple bole model. Forest. Chronicle 49 (3), 136–138.
Ounekham, K, 2009. Developing Volume and Taper Equations for Styrax tonkinensisin Laos. M. Sc. Thesis. University of Canterbury, NewZealand, p. 90.
Özçelik, R, Brooks, JR, 2012. Compatible volume and taper models for economically important tree species of Turkey. Ann. For. Sci. 69 (1), 105–118.
Pain, O, Boyer, E, 1996. A whole individual tree growth model for Norway spruce. In: Proceedings of the second Workshop "Connection between silviculture and wood quality through modelling approaches and simulation software. South Africa, pp. 13–23.
Paudyal, D, 2008. Sustainable resin tapping in Nepal: challenges and opportunities (A case from Salyan District). Initiation 2 (1), 172–179.
Pinheiro, J, Bates, D, 2000. Mixed-Effects Models in S and S-PLUS. Springer Science & Business Media.

Pinheiro J, Bates D, DebRoy S, Sarkar D, R Core Team (2018) NLME: linear and nonlinear mixed effects models. R package version 3.1-137, URL: https://CRAN.R-project.org/package=nlme.

Poudel, KP, Temesgen, H, Gray, AN, 2018. Estimating upper stem diameters and volume of Douglas-fir and Western hemlock trees in the Pacific Northwest. For. Ecosyst. 5, 1–12.

Core Team, R, 2021. R: A Language and Environment for Statistical Computing. R foundation for statistical computing, Vienna, Austria. URL. https://www.R-project.org/.

Rana, B.S., Singh, S.P., Singh, R.P., 1989. Biomass and net primary productivity in Central Himalayan forests along an altitudinal gradient. For. Ecol. Manage 27 (3-4), 199–218.

Rautiainen, O, 1992. Observations on the growth of planted *Pinus roxburghii* on high-quality sites in Kathmandu Valley. Banko Janakari 3 (3), 37–42.

Riemer, T, von, Gadow K, Slodoba, B, 1995. Ein Modell zurBeschreibung von Baumscha̎ften. AllgForstJagdztg 166 (7), 144–147.

Rojo, A, Perales, X, Sánchez-Rodríguez, F, Álvarez-González, JG, Gadow, KV, 2005. Stem taper functions for maritime pine (*Pinus pinaster*Ait.) in Galicia (Northwestern Spain). Eur. J. For. Res. 124, 177–186.

Sabatia, CO, Burkhart, HE, 2015. On the use of upper stem diameters to localize a segmented taper equation to new trees. For. Sci. 61 (3), 411–423.

Saud, P, Lynch, TB, KC, A, Guldin, JM, 2016. Using quadratic mean diameter and relative spacing index to enhance height–diameter and crown ratio models fitted to longitudinal data. Forestry 89 (2), 215–229.

Saud, P., Lynch, T.B., Cram, D.S., Guldin, J.M., 2019. An annual basal area growth model with multiplicative climate modifier fitted to longitudinal data for shortleaf pine. Forestry: Int. J. For. Res. 92 (5), 538–553.

Sharma, E. R., & Pukkala, T. (1990). Volume and biomass prediction equations of forest trees of Nepal. *Forest Survey and Statistical Division. Ministry of Forest and Soil Conservation, Kathmandu, Nepal*.

Sharma, KP, Bhatta, SP, Khatri, GB, Pajiyar, A, Joshi, DK, 2020. Estimation of carbon stock in the chir pine (*Pinus roxburghii* Sarg.) plantation forest of Kathmandu Valley, Central Nepal. J. For. Environ. Sci. 36 (1), 37–46.

Sharma, M, Oderwald, RG, 2001. Dimensionally compatible volume and taper equations. Canadian J. For. Res. 31 (5), 797–803.

Sharma, M, Parton, J, 2009. Modelling stand density effects on taper for jack pine and black spruce plantations using dimensional analysis. For. Sci. 55, 268–282.

Sharma, M, Zhang, SY, 2004. Variable-exponent taper equations for jack pine, black spruce, and balsam fir in eastern Canada. For. Ecol. Manage 198 (1-3), 39–53.

Sharma, RP, 2009. Modelling height-diameter relationship for Chir pine trees. Banko Janakari. 19 (2), 3–9.

Sigdel, SR, Dawadi, B, Camarero, JJ, Liang, E, Leavitt, SW, 2018. Moisture-limited tree growth for a subtropical Himalayan conifer forest in Western Nepal. Forests. 9 (6), 340.

Singh, A, Kushwaha, SPS, 2011. Refining logistic regression models for wildlife habitat suitability modeling a case study with muntjak and goral in the Central Himalayas, India. Ecol. Model. 222 (8), 1354–1366.

Tenzin, J, Wangchuk, T, Hasenauer, H, 2017. Form factor functions for nine commercial tree species in Bhutan. Forestry: Int. J. For. Res. 90 (3), 359–366.

Thapa, TB, Upadhyaya, CP, Timilsina, YP, Bhandari, SK, Puri, L, 2013. Predicting total height from diameter using nonlinear models in Pinus roxburghii. Nepal J. Sci. Technol. 14 (1), 147–152.

Tiwari, A, Thapa, N, Aryal, S, Rana, P, Adhikari, S, 2020. Growth performance of planted population of *Pinus roxburghii* in central Nepal. J. Ecol. Environ. 44, 1–11.

Trincado, G, Burkhart, HE, 2006. A generalized approach for modeling and localizing stem profile curves. For. Sci. 52 (6), 670–682.

Ulak, S, Ghimire, K, Gautam, R, Bhandari, SK, Poudel, KP, Timilsina, YP, Pradhan, D, Subedi, T, 2022. Predicting the upper stem diameters and volume of a tropical dominant tree species. J. For. Res. 33 (6), 1725–1737.

Valenti, MA, Cao, QV, 1986. Use of crown ratio to improve loblolly pine taper equations. Canadian J. For. Res. 16 (5), 1141–1145.

Valentine, HT, Gregoire, TG, 2001. A switching model of bole taper. Can. J. For. Res. 31 (8), 1400–1409.

Yang, Y, Huang, S, Trincado, G, Meng, SX, 2009. Nonlinear mixed-effects modeling of variable-exponent taper equations for lodgepole pine in Alberta, Canada. Eur. J. For. Res. 128, 415–429.

Zhao, D, Kane, M, 2017. New variable-top merchantable volume and weight equations derived directly from cumulative relative profiles for loblolly pine. For. Sci. 63 (3), 261–269.

Zhao, D, Lynch, TB, Westfall, J, Coulston, J, Kane, M, Adams, DE, 2019. Compatibility, development, and estimation of taper and volume equation systems. For. Sci. 65 (1), 1–13.